

Development of a New Free Radical Absorption Capacity Assay Method for Antioxidants: Aroxyl Radical Absorption Capacity (ARAC)

Shin-ichi Nagaoka,* Kanae Nagai, Yuko Fujii, Aya Ouchi, and Kazuo Mukai*

Department of Chemistry, Faculty of Science and Graduate School of Science and Engineering, Ehime University, Matsuyama 790-8577, Japan

S Supporting Information

ABSTRACT: A new free radical absorption capacity assay method is proposed with use of an aroxyl radical (2,6-di-*tert*-butyl-4-(4'-methoxyphenyl)phenoxy radical) and stopped-flow spectroscopy and is named the aroxyl radical absorption capacity (ARAC) assay method. The free radical absorption capacity (ARAC value) of each tocopherol was determined through measurement of the radical-scavenging rate constant in ethanol. The ARAC value could also be evaluated through measurement of the half-life of the aroxyl radical during the scavenging reaction. For the estimation of the free radical absorption capacity, the aroxyl radical was more suitable than the DPPH radical, galvinoxyl, and *p*-nitrophenyl nitronyl nitroxide. The ARAC value in tocopherols showed the same tendency as the free radical absorption capacities reported previously, and the tendency was independent of an oxygen radical participating in the scavenging reaction and of a medium surrounding the tocopherol and oxygen radical. The ARAC value can be directly connected to the free radical-scavenging rate constant, and the ARAC method has the advantage of treating a stable and isolable radical (aroxyl radical) in a user-friendly organic solvent (ethanol). The ARAC method was also successfully applied to a palm oil extract. Accordingly, the ARAC method would be useful in free radical absorption capacity assay of antioxidative reagents and foods.

KEYWORDS: aroxyl radical, scavenging rate, tocopherol, ARAC value, kinetic study

INTRODUCTION

Measurement and use of antioxidant capacity are topics of current interest not only in basic science communities but also in the food, pharmaceutical, and cosmetic industries.^{1–5} A reason for this is that reactive oxygen and nitrogen species such as free radicals and singlet oxygen play important roles in aging and disease.^{6–9} The oxygen radical absorbance capacity (ORAC) assay method^{1–4} had been most widely used to assess antioxidant capacity against free radicals. However, in 2012 the Agricultural Research Service of the U.S. Department of Agriculture (USDA) reported, “Recently the USDA’s Nutrient Data Laboratory (NDL) removed the USDA ORAC Database for Selected Foods from the NDL website due to mounting evidence that the values indicating antioxidant capacity have no relevance to the effects of specific bioactive compounds, including polyphenols on human health”.¹⁰ Accordingly, several alternative methods have been proposed to assess the antioxidant capacity against free radicals.^{8,11}

On the other hand, with respect to singlet oxygen, we proposed a method of assessing the antioxidant capacity and named it the singlet-oxygen absorption capacity (SOAC) assay method.⁵ The SOAC method was successfully applied to singlet-oxygen quenching antioxidants including carotenoids, tocopherols (TocHs), and polyphenols and also to vegetable extracts. However, with respect to free radicals we have not yet started developing a method of assessing the antioxidant capacity, although total estimation of the antioxidant capacity against free radicals and singlet oxygen is necessary. Instead, we performed kinetic studies of antioxidant reactions by using stopped-flow spectroscopy.^{12–15} In these previous studies, we determined the second-order rate constants (k_s values) of

reactions scavenging an aroxyl radical (2,6-di-*tert*-butyl-4-(4'-methoxyphenyl)phenoxy radical, ArO•) by TocHs, polyphenols, vitamin C, and so on in organic solvents, micellar solutions, and liposome membranes. ArO• is stable and can easily be isolated.

In the present paper, on the basis of our previous kinetic studies, we propose a new free radical absorption capacity assay method with use of ArO• and stopped-flow spectroscopy and name it the aroxyl radical absorption capacity (ARAC) assay method after ORAC. The ARAC value obtained here is directly connected to the k_s value. We also discuss possibilities of using various media and various radicals besides ArO• in the estimation of the free radical absorption capacity. Furthermore, the ARAC method is applied to a palm oil extract.

MATERIALS AND INSTRUMENTS

The structures of molecules used in this work are shown in Chart 1. α -, β -, γ -, and δ -TocHs were kindly supplied by Eisai Co., Ltd. 1,1-Diphenyl-2-picrylhydrazyl (DPPH•), *p*-nitrophenyl nitronyl nitroxide (2-(4-nitrophenyl)-4,4,5,5-tetramethylimidazole-3-oxide-1-oxyl, *p*-NPNN•), and guaranteed-grade ethanol (EtOH) were respectively obtained from Wako Pure Chemical Industries, Tokyo Chemical Industry, and Nacalai Tesque, and used without further purification.

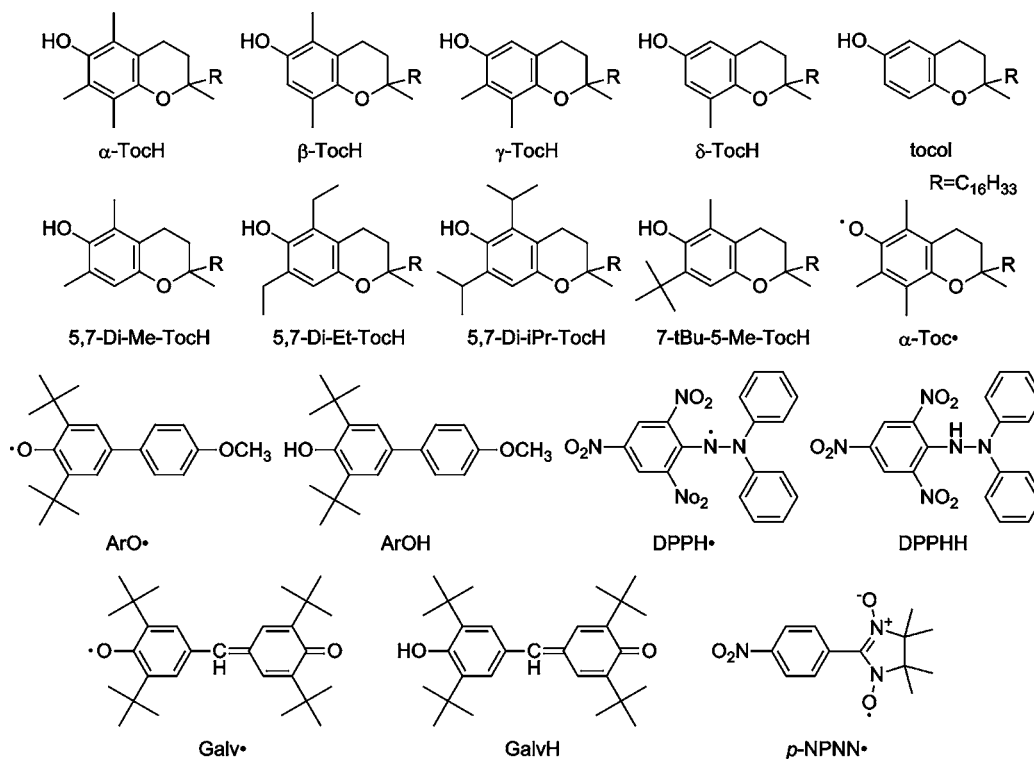
Because commercially available galvinoxyl (4-[[3,5-bis(1,1-dimethylethyl)-4-oxo-2,5-cyclohexadien-1-ylidene]methyl]-2,6-bis(1,1-dimethylethyl)phenoxy, Galv•) contained some impurities, it was synthesized anew from 2,6-di-*tert*-butylphenol according to the

Received: June 27, 2013

Revised: September 17, 2013

Accepted: September 24, 2013

Published: September 24, 2013

Chart 1. Molecular Structures of TocHs, α -Toc \cdot , ArO \cdot , ArOH, DPPH \cdot , DPPHH, Galv \cdot , GalvH, and *p*-NPNN \cdot 

method reported previously.^{16,17} Its purity was estimated to be 98% through measurement of molar magnetic susceptibility¹⁸ by using the superconducting quantum interference device (SQUID) method, which is a generally accepted method of determining the purity of a stable radical crystal. ArO \cdot and 2,6-di-*tert*-butyl-4-(4'-methoxyphenyl)phenol (ArOH) were prepared as reported in a previous paper.¹⁹ 1,1-Diphenyl-2-picrylhydrazine (DPPHH) and 4-[[3,5-bis(1,1-dimethylethyl)-4-oxo-2,5-cyclohexadien-1-ylidene]methyl]-2,6-bis(1,1-dimethylethyl)phenol (GalvH) were synthesized according to the methods reported previously.^{20,21} Tocol, 5,7-dimethyltolcol (5,7-Di-Me-TocH), 5,7-diethyltolcol (5,7-Di-Et-TocH), 5,7-diisopropyltolcol (5,7-Di-iPr-TocH), and 7-*tert*-butyl-5-methyltolcol (7-tBu-5-Me-TocH) were also prepared as reported previously.^{22,23} A palm oil extract used in the present study was kindly supplied by Tama Biochemical Co., Ltd., and called palm oil extract 5 (POES), the TocH content of which was given in a previous paper.²⁴

Kinetic data of free-radical scavenging reactions in EtOH were obtained by using a Unisoku RSP-1000-03F stopped-flow spectrophotometer. The apparatus and experimental method of the stopped-flow spectroscopy had previously been described in detail.^{25a} The measurement was performed under a nitrogen atmosphere at 25 °C. ArO \cdot was somewhat unstable at high temperature, and the stopped-flow spectrophotometer did not necessarily make a smooth solution-mixing at low temperature. Before the kinetic analyses, absorption decay curves of the radicals were corrected for the time-dependent background of the spectrometer.

RESULTS AND DISCUSSION

ARAC Method. Basically, on the basis of the second-order rate constant (k_s) of the following reaction, we estimate the ARAC value of an antioxidative reagent (AOH).



Here, AO \cdot denotes the phenoxyl radical produced from AOH. Reaction 1 is traced by measuring absorbance of ArO \cdot . Although the solution during reaction 1 is a four-component mixture, AOH studied in the present study shows no

absorption peak in the wavelength region longer than 300 nm, and absorption of unstable AO \cdot is generally weak or negligible. Furthermore, absorption peaks of ArO \cdot and ArOH do not overlap with each other as shown in Figure 1a.²⁶ Accordingly, absorption decays due to ArO \cdot consumption in reaction 1 can be measured without disturbance from any absorption change due to the other components in the solution.

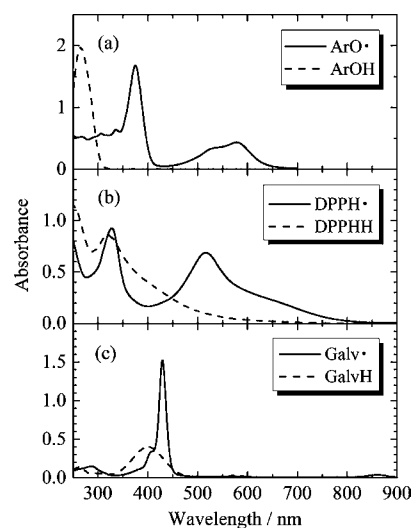


Figure 1. Absorption spectra of free radical and its product by antioxidant reaction with AOH: (a) ArO \cdot and ArOH. ²⁶ [ArO \cdot] = [ArOH] = 1.00×10^{-4} M. (b) DPPH \cdot and DPPHH. [DPPH \cdot] = [DPPHH] = 6.59×10^{-5} M. (c) Galv \cdot and GalvH. [Galv \cdot] = [GalvH] = 1.29×10^{-5} M. The solid and broken curves respectively denote the spectra of the free radical and its product in EtOH at room temperature.

This is an advantage of the use of ArO^\bullet in the estimation of free radical absorption capacity.

In reaction 1, equal volumes of EtOH solutions of AOH and ArO^\bullet were mixed with a stopped-flow spectrophotometer. Reaction 1 was studied under pseudo-first-order conditions ($[\text{AOH}] \gg [\text{ArO}^\bullet]$, where the brackets [] indicate molar concentration). $[\text{ArO}^\bullet]$ at the solution mixing was prepared so that the absorbance at 376 nm ($\epsilon = 16900 \text{ M}^{-1} \text{ cm}^{-1}$,²⁶) was 0.8–1 ($\sim 5\text{--}6 \times 10^{-5} \text{ M}$). The $[\text{AOH}]$ value was chosen so that the $[\text{ArO}^\bullet]$ would not largely decrease from the initial concentration within the short period of time (10–20 ms) required to completely mix AOH with ArO^\bullet and to make the solution homogeneous. A possibility of using another radical and/or medium in the estimation of free radical absorption capacity will be discussed in later sections. The ARAC estimation for POES, that is, the estimation in the case that the molar concentration is not clearly defined, will also be discussed in a later section.

A change in absorption spectrum measured during reaction 1 for $\alpha\text{-TocH}$ ($\text{AOH} = \alpha\text{-TocH}$) is shown in Figure 2a.²⁷ Although ArO^\bullet in EtOH was stable in the absence of $\alpha\text{-TocH}$ (see the solid curve given in Figure 2b), when an EtOH solution containing excess $\alpha\text{-TocH}$ was added to the solution

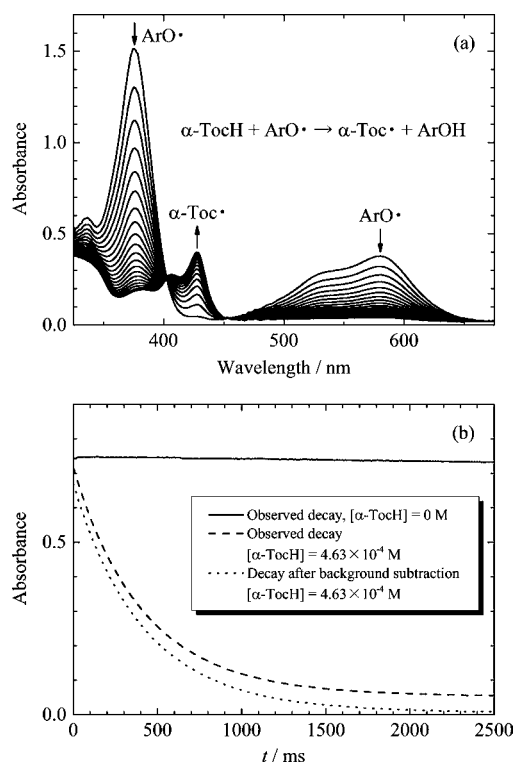


Figure 2. (a) Change in absorption spectrum observed at 60 ms intervals during reaction of $\alpha\text{-TocH}$ with ArO^\bullet in EtOH at 25 °C (reaction 1, $\text{AOH} = \alpha\text{-TocH}$).²⁷ The prepared $[\alpha\text{-TocH}]$ is 0.738 mM. The arrows indicate a decrease and an increase in absorbance of ArO^\bullet and $\alpha\text{-Toc}^\bullet$, respectively. (b) Absorbance decay of ArO^\bullet observed at 376 nm and 25 °C in EtOH during reaction 1 with $\alpha\text{-TocH}$. The solid curve denotes the natural decay in the absence of $\alpha\text{-TocH}$ ($[\alpha\text{-TocH}] = 0 \text{ M}$), and the other curves refer to the decay at prepared $[\alpha\text{-TocH}] = 4.63 \times 10^{-4} \text{ M}$. The solid and broken curves show the observed decays, and the dotted curve indicates the decay after background subtraction from the observed decay (broken curve). The broken and dotted curves were used to obtain the $k_{\text{obsd}}^{\alpha\text{-TocH}}$ and $t_{1/2}^{\alpha\text{-TocH}}$ values, respectively.

containing ArO^\bullet , the ArO^\bullet absorption peaks disappeared immediately, a peak of $\alpha\text{-tocopheroxyl}$ radical ($\alpha\text{-Toc}^\bullet$) appeared, and the isosbestic points were observed (Figure 2a). The peak of $\alpha\text{-Toc}^\bullet$ was weak and did not extensively overlap with that of ArO^\bullet . The broken curve given in Figure 2b shows the absorbance decay of ArO^\bullet at 376 nm during reaction 1 with $\alpha\text{-TocH}$. As seen from the initial difference between the solid and broken curves in Figure 2b, the decrease in ArO^\bullet absorbance during a period required to completely mix $\alpha\text{-TocH}$ with ArO^\bullet and to make the solution homogeneous was very small (0.026). Although some weak background absorbance (A_b) from species other than ArO^\bullet (e.g., $\alpha\text{-Toc}^\bullet$) was observed at 376 nm, the decay of the ArO^\bullet peak toward the background absorbance was well-characterized as a single-exponential decay and accelerated as $[\alpha\text{-TocH}]$ increased (see eqs 2 and 4 below). Furthermore, the decay rate at 376 nm is close to that at 580 nm,²⁸ where background absorbance from species other than ArO^\bullet is negligible (Figure 2a). Accordingly, the background disturbance at 376 nm is unlikely to have a great influence on our analyses. Similar results were also obtained for AOHs given in Chart 1.

When the absorbance due to ArO^\bullet is A_0 at the solution mixing ($t = 0$), the absorbance observed at a later time t ($A(t)$) is given as

$$A(t) = A_0 \exp(-k_{\text{obsd}}^{\text{AOH}} t) + A_b \quad (2)$$

where $k_{\text{obsd}}^{\text{AOH}}$ denotes the pseudo-first-order rate constant of reaction 1 and $A_0 \exp(-k_{\text{obsd}}^{\text{AOH}} t)$ is proportional to $[\text{ArO}^\bullet]$ at t . From the decay of the ArO^\bullet peak (e.g., broken curve given in Figure 2b), the $k_{\text{obsd}}^{\text{AOH}}$ value can be evaluated by using a standard least-squares analysis, in which subtraction of A_b is automatically made with the software used.

The experimental equation for $[\text{ArO}^\bullet]$ is given as

$$-d[\text{ArO}^\bullet] dt = k_{\text{obsd}}^{\text{AOH}} [\text{ArO}^\bullet] \quad (3)$$

The rate equation of reaction 1 and natural decay of ArO^\bullet is expressed as

$$-d[\text{ArO}^\bullet] dt = (k_0 + k_s^{\text{AOH}} [\text{AOH}]) [\text{ArO}^\bullet] \quad (4)$$

where k_0 stands for the first-order rate constant for the natural decay of ArO^\bullet in EtOH and k_s^{AOH} denotes the second-order rate constant of reaction 1 for AOH. Accordingly, $k_{\text{obsd}}^{\text{AOH}}$ in eq 3 is given by

$$k_{\text{obsd}}^{\text{AOH}} = k_0 + k_s^{\text{AOH}} [\text{AOH}] \quad (5)$$

where k_0 is much less than $k_s^{\text{AOH}} [\text{AOH}]$ under our experimental conditions. The open circles given in Figure 3 show the dependence of $\alpha\text{-TocH}$'s pseudo-first-order rate constant ($k_{\text{obsd}}^{\alpha\text{-TocH}}$) on prepared $[\alpha\text{-TocH}]$ in reaction 1 ($\text{AOH} = \alpha\text{-TocH}$). Because $[\text{AOH}]$ is nearly constant during reaction 1 under pseudo-first-order conditions ($[\text{AOH}] \gg [\text{ArO}^\bullet]$), k_s^{AOH} can be evaluated from the slope of the plot of $k_{\text{obsd}}^{\text{AOH}}$ versus $[\text{AOH}]$. The k_s^{AOH} values thus obtained are listed in Table 1, together with those reported previously.^{23,29,30}

The ARAC value of AOH is defined in the following equation and listed in Table 1.

$$\text{ARAC value} = k_s^{\text{AOH}} / k_s^{\alpha\text{-TocH}} \quad (6)$$

where $k_s^{\alpha\text{-TocH}}$ denotes the second-order rate constant of reaction 1 for $\alpha\text{-TocH}$. The ARAC value is a quantity without a unit and directly connected to the second-order rate constants (k_s^{AOH} and $k_s^{\alpha\text{-TocH}}$) of the free radical scavenging reactions

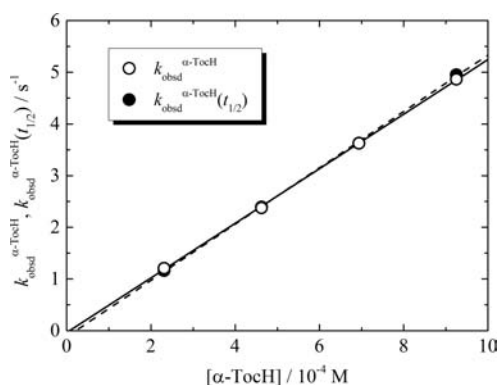


Figure 3. Dependences of $k_{\text{obsd}}^{\alpha\text{-TocH}}$ and $k_{\text{obsd}}^{\alpha\text{-TocH}}(t_{1/2})$ on prepared $[\alpha\text{-TocH}]$ in reaction 1 ($\text{AOH} = \alpha\text{-TocH}$). The open and solid circles respectively denote the plots of $k_{\text{obsd}}^{\alpha\text{-TocH}}$ and $k_{\text{obsd}}^{\alpha\text{-TocH}}(t_{1/2})$, and the solid and broken lines refer to the results of linear least-squares fitting. The plots of $k_{\text{obsd}}^{\alpha\text{-TocH}}$ and $k_{\text{obsd}}^{\alpha\text{-TocH}}(t_{1/2})$ were respectively used to obtain the $k_s^{\alpha\text{-TocH}}$ and $k_s^{\alpha\text{-TocH}}(t_{1/2})$ values given in Table 1

Table 1. k_s^{AOH} , ARAC, $k_s^{\text{AOH}}(t_{1/2})$, and ARAC ($t_{1/2}$) Values Obtained from Absorption Decay of ArO^\bullet during Reaction 1 with AOH in EtOH at 25 °C

AOH	$k_s^{\text{AOH}} \text{ M}^{-1} \text{ s}^{-1}$	ARAC value	$k_s^{\text{AOH}}(t_{1/2}) \text{ M}^{-1} \text{ s}^{-1}$	ARAC ($t_{1/2}$) value
$\alpha\text{-TocH}$	$5.12 \times 10^{3,a}$	1.00	5.45×10^3	1.00
$\beta\text{-TocH}$	$2.77 \times 10^{3,a}$	0.541	2.57×10^3	0.472
$\gamma\text{-TocH}$	$2.82 \times 10^{3,a}$	0.551	2.64×10^3	0.484
$\delta\text{-TocH}$	1.02×10^3	0.199	9.66×10^2	0.177
Tocol	$0.56 \times 10^{3,b}$	0.109		
5,7-Di-Me-TocH	$2.39 \times 10^{3,c}$	0.467		
5,7-Di-Et-TocH	$2.48 \times 10^{3,d}$	0.385		
5,7-Di-iPr-TocH	$2.51 \times 10^{3,c}$	0.490		
7-tBu-5-Me-TocH	$2.97 \times 10^{3,c}$	0.580		

^aThe measurement was carried out several times, and the average value is listed. ^bValue reported in ref 29. ^cValue reported in ref 23. ^dValue reported in ref 30.

(reaction 1). As shown in a later section, the ARAC value thus estimated can be conveniently compared with the data reported previously. ARAC estimation on the basis of the half-life of ArO^\bullet will be discussed in the next section.

ARAC Estimation Based on Half-Life of ArO^\bullet . In the measurement of free radical absorption capacity of foods and dietary supplements, evaluation of the half-life of ArO^\bullet reacting with AOH ($t_{1/2}^{\text{AOH}}$) may be more intuitive and convenient than that of $k_{\text{obsd}}^{\text{AOH}}$, because similar half-life evaluation has been frequently used in the field.^{31,32} Accordingly, in this section, we try to estimate the ARAC values on the basis of $t_{1/2}^{\text{AOH}}$.

When A_b is seen in the absorbance decay curve of ArO^\bullet at 376 nm during reaction 1 (see the broken curve given in Figure 2b), subtraction of A_b (background subtraction) is needed before the $t_{1/2}^{\text{AOH}}$ evaluation. By using $t_{1/2}^{\text{AOH}}$ obtained after the subtraction, the pseudo-first-order rate constant of reaction 1 for AOH ($k_{\text{obsd}}^{\text{AOH}}(t_{1/2})$) is expressed in the following way:^{25b}

$$k_{\text{obsd}}^{\text{AOH}}(t_{1/2}) = \ln 2 / t_{1/2}^{\text{AOH}} \quad (7)$$

Figure 3 shows the dependence of $k_{\text{obsd}}^{\alpha\text{-TocH}}(t_{1/2})$ on prepared $[\alpha\text{-TocH}]$ in reaction 1 ($\text{AOH} = \alpha\text{-TocH}$), together

with that of $k_{\text{obsd}}^{\alpha\text{-TocH}}$ given in the preceding section, and it is seen that $k_{\text{obsd}}^{\text{AOH}}(t_{1/2})$ can be expressed as

$$k_{\text{obsd}}^{\text{AOH}}(t_{1/2}) = k_0 + k_s^{\text{AOH}}(t_{1/2})[\text{AOH}] \quad (8)$$

where $k_s^{\text{AOH}}(t_{1/2})$ means the second-order rate constant estimated on the basis of $t_{1/2}^{\text{AOH}}$ and is obtained from the slope of the plot of $k_{\text{obsd}}^{\text{AOH}}(t_{1/2})$ versus $[\text{AOH}]$. The free radical absorption capacity of AOH on the basis of $t_{1/2}^{\text{AOH}}$ is defined in the following equation (ARAC ($t_{1/2}$) value):

$$\text{ARAC} (t_{1/2}) \text{ value} = k_s^{\text{AOH}}(t_{1/2}) / k_s^{\alpha\text{-TocH}}(t_{1/2}) \quad (9)$$

The $k_s^{\text{AOH}}(t_{1/2})$ and ARAC ($t_{1/2}$) values thus obtained are listed in Table 1. These values are comparable with the k_s^{AOH} and ARAC values obtained in the preceding section. Thus, the second-order rate constant of reaction 1 and the free radical absorption capacity of AOH may be estimated through the measurement of $t_{1/2}^{\text{AOH}}$ as well as through that of $k_{\text{obsd}}^{\text{AOH}}$ given in the preceding section. However, $t_{1/2}^{\text{AOH}}$ is evaluated basically from two experimental points (time difference between A_0 and $A_0/2$), whereas $k_{\text{obsd}}^{\text{AOH}}$ is evaluated by using a least-squares analysis for many experimental points. Furthermore, the simple background subtraction at a guess may yield an error in $t_{1/2}^{\text{AOH}}$. Accordingly, the $k_s^{\text{AOH}}(t_{1/2})$ and ARAC ($t_{1/2}$) values are less reliable than the k_s^{AOH} and ARAC values obtained in the preceding section.

However, similar half-life evaluation has been used so far in antioxidant capacity assays,^{31,32} because conveniently the product of the half-life and the antioxidant concentration then prepared is inversely proportional to the antioxidant efficiency (see DPPH assay section of ref 32). In fact, because k_0 is negligible as seen from the intercept of $k_{\text{obsd}}^{\alpha\text{-TocH}}(t_{1/2})$ versus $[\alpha\text{-TocH}]$ plot in Figure 3, by using eqs 7 and 8, the second-order rate constant estimated on the basis of $t_{1/2}^{\text{AOH}}$ under $k_0 = 0$ ($k_s^{\text{AOH}}(t_{1/2}, k_0 = 0)$) can be expressed as

$$k_s^{\text{AOH}}(t_{1/2}, k_0 = 0) = \ln 2 / t_{1/2}^{\text{AOH}}[\text{AOH}] \quad (10)$$

where $[\text{AOH}]$ denotes the molar concentration of AOH prepared for the $t_{1/2}^{\text{AOH}}$ measurement. Equation 9 is then rewritten as

$$\begin{aligned} \text{ARAC} (t_{1/2}, k_0 = 0) \text{ value} \\ = t_{1/2}^{\alpha\text{-TocH}}[\alpha\text{-TocH}] / t_{1/2}^{\text{AOH}}[\text{AOH}] \end{aligned} \quad (11)$$

Accordingly, even without k_s^{AOH} and $k_s^{\alpha\text{-TocH}}$, the ARAC ($t_{1/2}, k_0 = 0$) value can be evaluated from $t_{1/2}^{\text{AOH}}$, $t_{1/2}^{\alpha\text{-TocH}}$, $[\text{AOH}]$, and $[\alpha\text{-TocH}]$. The ARAC ($t_{1/2}, k_0 = 0$) values thus obtained are given in the Supporting Information.

As shown in Figure 3, four absorbance decay curves of ArO^\bullet are necessary for obtaining the $k_s^{\alpha\text{-TocH}}$ value, and in total eight curves, are generally measured in the k_s^{AOH} and $k_s^{\alpha\text{-TocH}}$ estimation, that is, the ARAC estimation in eq 6. On the other hand, the $t_{1/2}^{\alpha\text{-TocH}}$ value can be obtained from only one decay curve of ArO^\bullet , and $[\alpha\text{-TocH}]$ is the molar concentration of $\alpha\text{-TocH}$ prepared for the $t_{1/2}^{\alpha\text{-TocH}}$ measurement. Therefore, measurement of two curves in total is enough for the evaluation of $t_{1/2}^{\text{AOH}}$, $t_{1/2}^{\alpha\text{-TocH}}$, $[\text{AOH}]$, and $[\alpha\text{-TocH}]$, that is, for the ARAC ($t_{1/2}, k_0 = 0$) estimation in eq 11. Like this, one can save time and trouble through the half-life evaluation in the ARAC method, although the ARAC ($t_{1/2}, k_0 = 0$) value thus obtained is less reliable than the ARAC value obtained in the preceding section.

Possibility of Using a Radical Other than ArO• in Estimation of Free Radical Absorption Capacity. Because ArO• is not commercially available, in this section we examine the possibility of using a free radical other than ArO• in the estimation of the free radical absorption capacity of AOH. Although typical commercially available radicals are DPPH•, Galv•, and *p*-NPNN•, the purity should be checked before the measurement as noted in a previous section. As described below, ArO• is the most suitable for the estimation of the free radical absorption capacity of AOH.

DPPH•. The radical scavenging reaction for DPPH• by AOH is given as

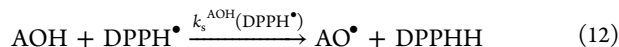


Figure 1b shows absorption spectra of DPPH• and DPPHH, whose concentrations are equal to each other. Absorption peaks of DPPH• and DPPHH overlap with each other around 325 nm, and a peak of DPPH• at 517 nm also overlaps with the tail of the absorption of DPPHH. Accordingly, as reported previously,³³ the rate constant estimation from absorption decay at 325 nm is difficult, and complex background subtraction from the decay curve is needed at 517 nm.

The absorption decay measurement at the above-mentioned troublesome overlap in DPPH• should be avoided in the estimation of the second-order rate constant of reaction 12 ($k_s^{\text{AOH}}(\text{DPPH}^{\bullet})$) and then the free radical absorption capacity of AOH (ARAC (DPPH•) value). Therefore, we tried to measure the decay in the wavelength region longer than 600 nm, because the tail of the absorption of DPPHH does not show strong intensity there. Nevertheless, extensive background subtraction is still needed in the DPPH• decay analysis for the estimation of the $k_s^{\text{AOH}}(\text{DPPH}^{\bullet})$ and ARAC (DPPH•) values. Furthermore, in DPPH•, the absorbance above 600 nm is much less than those at the absorption peaks. Accordingly, the $k_s^{\text{AOH}}(\text{DPPH}^{\bullet})$ and ARAC (DPPH•) values thus obtained are less reliable than the k_s^{AOH} and ARAC values obtained from the absorption decay of ArO• in a previous section, and therefore ArO• is more suitable than DPPH• for the estimation of the free radical absorption capacity of AOH.

The $k_s^{\text{AOH}}(\text{DPPH}^{\bullet})$ and ARAC (DPPH•) values thus obtained are listed in Table 2, together with those reported previously.³⁴ Because groups around the reactive site of DPPH•

Table 2. $k_s^{\text{AOH}}(\text{DPPH}^{\bullet})$ and ARAC (DPPH•) Values Obtained from Absorption Decay of DPPH• during Reaction 12 with AOH in EtOH at 25 °C and E_p

AOH	$k_s^{\text{AOH}}(\text{DPPH}^{\bullet})$ $\text{M}^{-1} \text{s}^{-1}$	ARAC (DPPH•) value ^a	E_p ^b mV vs SCE
α -TocH	358	1.00	860
β -TocH	149	0.416	920
γ -TocH	174	0.486	930
δ -TocH	64.2	0.179	990
tocol	42.0 ^c	0.117	1050
5,7-Di-Me-TocH	128 ^c	0.358	890
5,7-Di-Et-TocH	76.0 ^c	0.212	890
5,7-Di-iPr-TocH	46.0 ^c	0.128	890
7-t-Bu-5-Me-TocH	67.0 ^c	0.187	880

^aAlthough this is also called an ARAC value for the sake of consistency in the present paper, DPPH• is not an aroxyl radical. ^bValues reported in ref 23. ^cValues reported in ref 34.

(N•) are much bulkier³⁵ than those of ArO• (O•), the $k_s^{\text{AOH}}(\text{DPPH}^{\bullet})$ value of an AOH (Table 2) is generally less than the k_s^{AOH} value obtained from the absorption decay of ArO• during reaction 1 with the AOH (Table 1). The second-order rate constant and free radical absorption capacities obtained from the half-life of DPPH• during reaction 12 are given in the Supporting Information.

Peak oxidation potentials (E_p values) of AOHs studied in this work²³ are listed in Table 2, together with the $k_s^{\text{AOH}}(\text{DPPH}^{\bullet})$ and ARAC (DPPH•) values. Figure 4 shows a semilog plot of

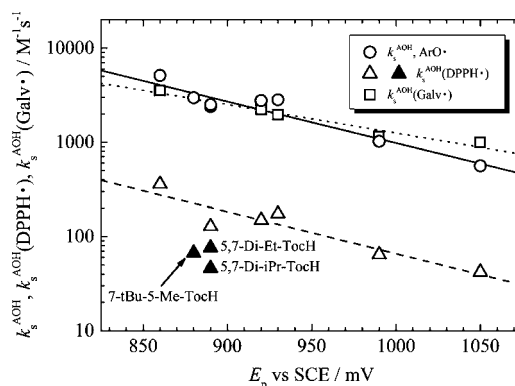


Figure 4. Semilog plots of k_s^{AOH} (circles), $k_s^{\text{AOH}}(\text{DPPH}^{\bullet})$ (triangles), and $k_s^{\text{AOH}}(\text{Galv}^{\bullet})$ (squares) versus E_p . The semilog plot of k_s^{AOH} gives a good linear fit with a slope of -4.40 V^{-1} , an intercept of $2.47 \times 10^7 \text{ M}^{-1} \text{ s}^{-1}$, and a correlation coefficient of -0.946 (solid line). Except for those of 5,7-Di-Et-TocH, 5,7-Di-iPr-TocH, and 7-t-Bu-5-Me-TocH (solid triangles), the semilog plot of $k_s^{\text{AOH}}(\text{DPPH}^{\bullet})$ gives a good linear fit with a slope of -4.44 V^{-1} , an intercept of $1.82 \times 10^6 \text{ M}^{-1} \text{ s}^{-1}$, and a correlation coefficient of -0.934 (open triangles and broken line). The semilog plot of $k_s^{\text{AOH}}(\text{Galv}^{\bullet})$ gives a good linear fit with a slope of -3.03 V^{-1} , an intercept of $1.33 \times 10^6 \text{ M}^{-1} \text{ s}^{-1}$, and a correlation coefficient of -0.980 (dotted line).

$k_s^{\text{AOH}}(\text{DPPH}^{\bullet})$ versus E_p , together with that of k_s^{AOH} obtained from the absorption decay of ArO•. Except for $k_s^{\text{AOH}}(\text{DPPH}^{\bullet})$ values of 5,7-Di-Et-TocH, 5,7-Di-iPr-TocH, and 7-t-Bu-5-Me-TocH, the plot for each of ArO• and DPPH• is found to be linear, and the slopes of the plots for ArO• and DPPH• are close to each other. The reason for this linear relationship was previously explained in terms of electron transfer and proton tunneling,¹³ which play important roles in free radical scavenging by natural polyphenols.³⁶ The above-mentioned exception in the $k_s^{\text{AOH}}(\text{DPPH}^{\bullet})$ values of 5,7-Di-Et-TocH, 5,7-Di-iPr-TocH, and 7-t-Bu-5-Me-TocH is thought to come from a steric effect by bulky groups around the reactive sites of these TocHs and DPPH•. The bulky groups (ethyl, isopropyl, and *tert*-butyl groups) around the reactive site of 5,7-Di-Et-TocH, 5,7-Di-iPr-TocH, and 7-t-Bu-5-Me-TocH (OH group) hinder reaction 12, together with the bulky groups around the reactive site of DPPH• (N•).³⁵ In contrast to reaction 12, such a steric effect is absent in reaction 1, because the groups around the reactive site of ArO• (O•) are much less bulky than those of DPPH• (N•).³⁵ Accordingly, for the estimation of the free radical absorption capacity of AOH, ArO• is, again, more suitable than DPPH•, because the free radical scavenging capacity against DPPH• is, in contrast to that against ArO•, underestimated for an AOH with some bulky groups around the reactive site.

Galv•. The radical-scavenging reaction for Galv• by AOH is given as

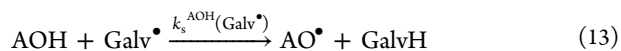


Figure 1c shows absorption spectra of Galv[•] and GalvH, the concentrations of which are equal to each other. An absorption peak of Galv[•] at 429 nm extensively overlaps with that of GalvH at 401 nm. Accordingly, the absorption decay measurement at 429 nm may induce some error in the rate constant estimation for reaction 13, although kinetic studies using Galv[•] were reported previously.³⁷ Thus, for the estimation of the free radical absorption capacity of AOH, ArO[•] is more suitable than Galv[•]. However, after extensive and careful background subtraction, the second-order rate constant of reaction 13 and then the free radical absorption capacity of AOH against Galv[•] were obtained ($k_s^{\text{AOH}}(\text{Galv}^{\bullet})$ and ARAC (Galv[•]) values, respectively) and are listed in Table 3. As

Table 3. $k_s^{\text{AOH}}(\text{Galv}^{\bullet})$ and ARAC (Galv[•]) Values Obtained from Absorption Decay of Galv[•] during Reaction 13 with AOH in EtOH at 25 °C

AOH	$k_s^{\text{AOH}}(\text{Galv}^{\bullet})/\text{M}^{-1} \text{s}^{-1}$	ARAC (Galv [•]) value
α -TocH	3.52×10^3	1.00
β -TocH	2.23×10^3	0.634
γ -TocH	1.96×10^3	0.557
δ -TocH	1.15×10^3	0.327
tocol	9.88×10^2	0.281

explained above, these values are less reliable than those obtained from the absorption decay of ArO[•] in a previous section, but the dependencies of the k_s^{AOH} and $k_s^{\text{AOH}}(\text{Galv}^{\bullet})$ values on E_p are similar to each other as shown in Figure 4. The second-order rate constant and free radical absorption capacities obtained from the half-life of Galv[•] during reaction 13 are given in the Supporting Information.

p -NPNN[•]. The radical scavenging reaction for p -NPNN[•] by AOH is given as

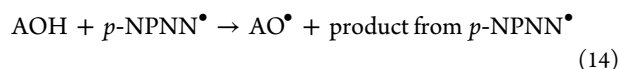


Figure 5 shows a change in absorption spectrum measured during reaction 14 for α -TocH (AOH = α -TocH). Despite the condition that $[\alpha\text{-TocH}]$ is greater than $[p\text{-NPNN}^{\bullet}]$ by as

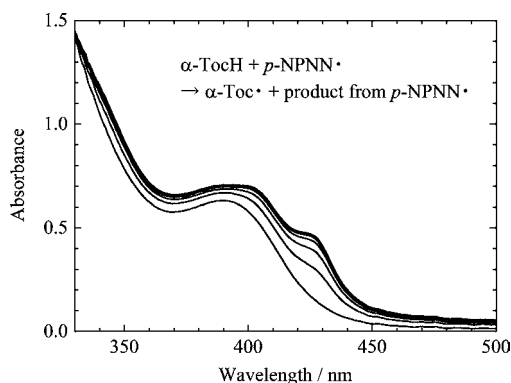


Figure 5. Change in absorption spectrum observed at 100 ms intervals during reaction of α -TocH with p -NPNN[•] in EtOH at 25 °C (reaction 14, AOH = α -TocH). The prepared $[\alpha\text{-TocH}]$ and $[p\text{-NPNN}^{\bullet}]$ are 1.16×10^{-1} and 1.80×10^{-4} M, respectively. After the reaction proceeds, two weak shoulders due to $\alpha\text{-Toc}^{\bullet}$ are seen at 428 and \sim 405 nm besides a peak of $p\text{-NPNN}^{\bullet}$ at 390 nm.

much as 3 orders of magnitude, the absorption change of p -NPNN[•] is too small to be used for the estimation of the rate constant of reaction 14 and then the free radical absorption capacity of AOH. Accordingly, p -NPNN[•] is not suitable for the estimation of the free radical absorption capacity of AOH. Similar results were also obtained for 2,2,6,6-tetramethylpiperidine 1-oxyl radicals (TEMPO[•]s). The reason for the very small absorption change of p -NPNN[•] is that p -NPNN[•] is much more stable than ArO[•], DPPH[•], and Galv[•]. The high stability of p -NPNN[•] comes from delocalization of the unpaired electron over the two NO groups^{38,39} and from resonance between $\text{N}=\text{O}^{\bullet}$ and $\text{N}^+=\text{O}^{\bullet-}$,⁴⁰ within each of the two NO groups.

Comparison with Previous Results. AOH's free radical absorption capacity corresponding to the ARAC value can also be derived from the ratio of AOH's previously reported free radical-scavenging rate constant or antioxidant efficiency to the corresponding α -TocH value, which should be determined under the same conditions as those applied to the AOH. In this section, the ARAC value estimated in the present study is compared with four ratios derived from previous studies,^{29,41–43} for which data are cited in a well-read review paper.⁴⁴ The free radical-scavenging rate constants of TocHs were previously obtained for the reactions with poly-(peroxystyryl)peroxyl radical in chlorobenzene⁴¹ and for those with ArO[•] in nonionic Triton X-100 micellar solution.²⁹ The antioxidant efficiencies of TocHs were previously obtained against peroxyl radical from linoleic acid in cationic HDTBr micellar solution⁴² and anionic SDS micellar solution.⁴³

Table 4 shows the above-mentioned four ratios for each TocH, together with the ARAC value estimated in this study.

Table 4. ARAC Value and Ratio of AOHs Previously Reported Free Radical-Scavenging Rate Constant or Antioxidant Efficiency to α -TocH's Corresponding Value Determined under the Same Conditions as Those Applied to AOH

AOH	ARAC value, present work ^a	ratio			
		ref 41 ^b	ref 29 ^c	ref 42 ^d	ref 43 ^e
α -TocH	1.00	1.0	1.00	1.00	1.0
β -TocH	0.541	0.41	0.21	0.548	0.59
γ -TocH	0.551	0.44	0.20	0.576	0.59
δ -TocH	0.199	0.14	0.029	0.299	0.24
tocol	0.109		0.0069		
5,7-Di-Me-TocH	0.467	0.56			

^aARAC values given in Table 1. ^bRatios derived from rate constants obtained for reactions of TocHs with poly(peroxystyryl)peroxyl radical in chlorobenzene at 30 °C by using an oxygen consumption method. ^cARAC values derived from those with ArO[•] in nonionic Triton X-100 micellar solution (5.0 wt %) at pH 7.0 and 25 °C by using stopped-flow spectroscopy. ^dRatios derived from antioxidant efficiencies against peroxyl radical coming from linoleic acid in cationic HDTBr micellar solution (0.10 M) at pH 7.4 and 37 °C by measuring absorbance of conjugated-diene-hydroperoxide formation at 234 nm. ^eRatios derived from those in anionic SDS micellar solution (0.5 M) by using an oxygen consumption method.

These ratios do not quantitatively agree with the ARAC value, because the ratios and the ARAC value depend on the oxygen radical participating in the scavenging reaction (ArO[•], poly-(peroxystyryl)peroxyl radical, or peroxyl radicals from linoleic acid) and on the medium surrounding the TocH and oxygen

radical (EtOH, chlorobenzene, or micellar solution). A reason for this dependence was described previously.²⁹ However, all of the ratios and the ARAC value given in Table 4 decrease in the order

$$\alpha\text{-TocH} > \beta\text{-TocH} \sim \gamma\text{-TocH} \sim 5,7\text{-Di-Me-TocH} > \delta\text{-TocH} > \text{tocol} \quad (15)$$

This result suggests that the tendency of the free radical absorption capacity in TocHs is independent of the radical and medium. Among these free radical absorption capacity assay methods, the ARAC method has the advantage of treating stable and isolable ArO• in user-friendly EtOH.

Furthermore, because the tendency (inequality 15) is consistent with biological activities of orally provided TocHs (fetal resorption assay),⁴⁵ the ARAC value of TocH can also be used as a measure of biological activity. Accordingly, the ARAC method would be useful in free radical absorption capacity assays of AOHs. The most important advantage of the ARAC method over various widely established assay methods^{31,32} is that the ARAC value can be directly connected to the free radical-scavenging rate constant as shown in eq 6. On the other hand, the shortcoming is that ArO• is not commercially available and a stopped-flow spectrophotometer is necessary.

Application to Palm Oil Extract. The antioxidant activity of foods and plant extracts has received considerable interest from food science communities.^{46,47} Accordingly, in this section, we apply the ARAC method to a palm oil extract (POES). As mentioned in a previous paper,²⁴ POES contains various AOHs with a variety of concentrations, and the AOHs react with ArO•. Because molar concentration corresponding to [AOH] in eq 5 cannot be clearly defined for POES, the concentration of POES is forced to be expressed in a unit of g L⁻¹ ([POES]_g). Accordingly, in the following equation corresponding to eq 5, the second-order rate constant for POES is shown in a unit of L g⁻¹ s⁻¹ ($k_s^{\text{POES(g)}}$).

$$k_{\text{obsd}}^{\text{POES}} = k_0 + k_s^{\text{POES(g)}}[\text{POES}]_g \quad (16)$$

where $k_{\text{obsd}}^{\text{POES}}$ denotes the pseudo-first-order rate constant for POES scavenging ArO•.

Figure 6 shows the dependence of $k_{\text{obsd}}^{\text{POES}}$ on prepared [POES]_g. From the slope of the plot of $k_{\text{obsd}}^{\text{POES}}$ versus [POES]_g, the $k_s^{\text{POES(g)}}$ value could be evaluated. The measure-

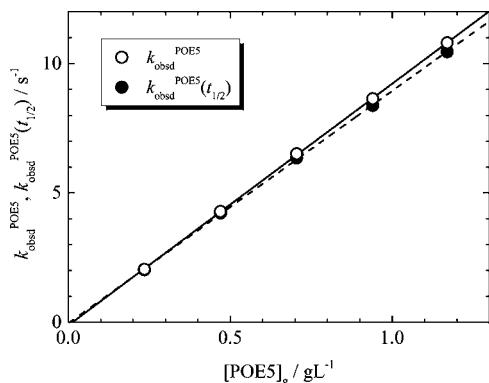


Figure 6. Dependences of $k_{\text{obsd}}^{\text{POES}}$ (open circles) and $k_{\text{obsd}}^{\text{POES}(t_{1/2})}$ (solid circles) on prepared [POES]_g. The solid and broken lines refer to the results of linear least-squares fitting. The plots of $k_{\text{obsd}}^{\text{POES}}$ and $k_{\text{obsd}}^{\text{POES}(t_{1/2})}$ were respectively used to obtain the $k_s^{\text{POES(g)}}$ and $k_s^{\text{POES(g)}(t_{1/2})}$ values given in the text.

ment was carried out three times, and the average $k_s^{\text{POES(g)}}$ value was 9.11 L g⁻¹ s⁻¹. Because the second-order rate constant shown in L g⁻¹ s⁻¹ for $\alpha\text{-TocH}$ ($k_s^{\alpha\text{-TocH(g)}}$) is equal to the ratio of the $k_s^{\alpha\text{-TocH}}$ value in M⁻¹ s⁻¹ (5.12×10^3) to the molecular weight of $\alpha\text{-TocH}$ (430.71), the $k_s^{\alpha\text{-TocH(g)}}$ value was calculated to be 11.9 L g⁻¹ s⁻¹. These second-order rate constants in L g⁻¹ s⁻¹ were used in the following equation corresponding to eq 6 to obtain the free radical absorption capacity of POES (ARAC (g) value).

$$\text{ARAC (g) value} = k_s^{\text{POES(g)}}/k_s^{\alpha\text{-TocH(g)}} \quad (17)$$

Finally, the ARAC (g) value of POES in eq 17 was obtained to be 0.766.

As well as in eq 7, the pseudo-first-order rate constant for POES on the basis of the half-life of ArO• ($k_{\text{obsd}}^{\text{POES}(t_{1/2})}$) can be expressed in the following way:

$$k_{\text{obsd}}^{\text{POES}(t_{1/2})} = \ln 2/t_{1/2}^{\text{POES}} \quad (18)$$

Here, $t_{1/2}^{\text{POES}}$ denotes the half-life of ArO• reacting with various AOHs involved in POES. Figure 6 shows the dependence of $k_{\text{obsd}}^{\text{POES}(t_{1/2})}$ on [POES]_g, together with that of $k_{\text{obsd}}^{\text{POES}}$ given above. In the figure the $k_{\text{obsd}}^{\text{POES}}$ value given in eq 16 is close to the $k_{\text{obsd}}^{\text{POES}(t_{1/2})}$ one in eq 18, and $k_{\text{obsd}}^{\text{POES}(t_{1/2})}$ can be expressed as

$$k_{\text{obsd}}^{\text{POES}(t_{1/2})} = k_0 + k_s^{\text{POES(g)}(t_{1/2})}[\text{POES}]_g \quad (19)$$

where $k_s^{\text{POES(g)}(t_{1/2})}$ means the second-order rate constant estimated on the basis of $t_{1/2}^{\text{POES}}$. From the slope of the plot of $k_{\text{obsd}}^{\text{POES}(t_{1/2})}$ versus [POES]_g, the $k_s^{\text{POES(g)}(t_{1/2})}$ value was evaluated to be 8.94 L g⁻¹ s⁻¹. The $k_s^{\alpha\text{-TocH(g)}(t_{1/2})}$ value was calculated to be 12.7 L g⁻¹ s⁻¹, and the free radical absorption capacity of POES on the basis of $t_{1/2}^{\text{POES}}$ (ARAC ($t_{1/2}$, g) value), which is given in eq 20, was 0.704.

$$\text{ARAC (}t_{1/2}\text{, g) value} = k_s^{\text{POES(g)}(t_{1/2})}/k_s^{\alpha\text{-TocH(g)}(t_{1/2})} \quad (20)$$

The ARAC ($t_{1/2}$, g) value of POES is comparable with the ARAC (g) value. The values corresponding to ARAC ($t_{1/2}, k_0 = 0$) are given in the Supporting Information.

Thus, it has been shown that the ARAC method can be applied to the palm oil extract. We attempt to extend the application to free radical scavenging action by various edible oils and food extracts. The ARAC method would be useful in free radical absorption capacity assays of foods in addition to the assays of AOHs.

■ ASSOCIATED CONTENT

● Supporting Information

Second-order rate constants and free radical absorption capacities obtained from half-lives of DPPH• and Galv• during reactions 12 and 13 with AOH, ARAC ($t_{1/2}, k_0 = 0$) values, and semilog plots of $A(t)$ versus t . This material is available free of charge via the Internet at <http://pubs.acs.org>.

■ AUTHOR INFORMATION

Corresponding Authors

* (S.N.) Phone: 81-89-927-9592. Fax: 81-89-927-9590. E-mail: nagaoka@ehime-u.ac.jp.

* (K.M.) Phone: 81-89-927-9588. Fax: 81-89-927-9590. E-mail: mukai-k@dpc.ehime-u.ac.jp

Funding

This work was partly supported by a Grant-in-Aid for Challenging Exploratory Research (No. 24658123) from the Japan Society for the Promotion of Science.

Notes

The authors declare no competing financial interest.

ACKNOWLEDGMENTS

We express our sincere thanks to Professor Kensuke Konishi, Dr. Kimiko Takamatsu, and Tsunagu Mochizuki of Ehime University for his measurement of the Galv[•] purity with SQUID, for her synthesis of DPPHH, and for his measurement of $k_s^{\text{A}^{\text{OH}}(\text{Galv}^{\bullet})}$ and ARAC (Galv[•]) values of β -TocH, respectively. We also thank Katsuhiko Izumisawa and Tomomi Suzuki of Eisai Co., Ltd., Taisuke Koike of Eisai Food and Chemical Co., Ltd., and Tama Biochemical, Co. Ltd. for their generous gifts of TocHs, crude palm oil, and POES.

REFERENCES

- (1) Cao, G.; Alessio, H. M.; Cutler, R. G. Oxygen-radical absorbance capacity assay for antioxidants. *Free Radical Biol. Med.* **1993**, *14*, 303–311.
- (2) Wang, H.; Cao, G.; Prior, R. L. Total antioxidant capacity of fruits. *J. Agric. Food Chem.* **1996**, *44*, 701–705.
- (3) Ou, B.; Hampsch-Woodill, M.; Prior, R. L. Development and validation of an improved oxygen radical absorbance capacity assay using fluorescein as the fluorescent probe. *J. Agric. Food Chem.* **2001**, *49*, 4619–4626.
- (4) Huang, D.; Ou, B.; Hampsch-Woodill, M.; Flanagan, J. A.; Deemer, E. K. Development and validation of oxygen radical absorbance capacity assay for lipophilic antioxidants using randomly methylated β -cyclodextrin as the solubility enhancer. *J. Agric. Food Chem.* **2002**, *50*, 1815–1821.
- (5) For part 3 in this series, see: Mukai, K.; Ouchi, A.; Takahashi, S.; Aizawa, K.; Inakuma, T.; Terao, J.; Nagaoka, S. Development of singlet oxygen absorption capacity (SOAC) assay method. 3. Measurements of the SOAC values for phenolic antioxidants. *J. Agric. Food Chem.* **2012**, *60*, 7905–7916.
- (6) *Healthy Aging for Functional Longevity*; Park, S. C., Hwang, E. S., Kim, H.-S., Park, W.-Y., Eds.; Annals of the New York Academy of Sciences 928; New York Academy of Sciences: New York, 2001.
- (7) *Increasing Healthy Life Span*; Harman, D., Ed.; Annals of the New York Academy of Sciences 959; New York Academy of Sciences: New York, 2002.
- (8) Niki, E. Assessment of antioxidant capacity *in vitro* and *in vivo*. *Free Radical Biol. Med.* **2010**, *49*, 503–515 (review) and references cited therein.
- (9) Finley, J. W.; Kong, A.-N.; Hintze, K. J.; Jeffery, E. H.; Ji, L. L.; Lei, X. G. Antioxidants in foods: state of the science important to the food industry. *J. Agric. Food Chem.* **2011**, *59*, 6837–6846.
- (10) U.S. Department of Agriculture, Agricultural Research Service. Oxygen Radical Absorbance Capacity (ORAC) of Selected Foods, release 2 (2010), <http://www.ars.usda.gov/services/docs.htm?docid=15866> (accessed Sept 2013).
- (11) Takashima, M.; Horie, M.; Shichiri, M.; Hagihara, Y.; Yoshida, Y.; Niki, E. Assessment of antioxidant capacity for scavenging free radicals *in vitro*: a rational basis and practical application. *Free Radical Biol. Med.* **2012**, *52*, 1242–1252 and references cited therein.
- (12) Mukai, K.; Fukuda, K.; Tajima, K.; Ishizu, K. A kinetic study of reactions of tocopherols with a substituted phenoxyl radical. *J. Org. Chem.* **1988**, *53*, 430–432.
- (13) Nagaoka, S.; Kuranaka, A.; Tsuboi, H.; Nagashima, U.; Mukai, K. Mechanism of antioxidant reaction of vitamin E. Charge transfer and tunneling effect in proton-transfer reaction. *J. Phys. Chem.* **1992**, *96*, 2754–2761.
- (14) Mitani, S.; Ouchi, A.; Watanabe, E.; Kanesaki, Y.; Nagaoka, S.; Mukai, K. Stopped-flow kinetic study of the aroxyl radical-scavenging

action of catechins and vitamin C in ethanol and micellar solutions. *J. Agric. Food Chem.* **2008**, *56*, 4406–4417.

(15) Fukuzawa, K.; Ouchi, A.; Shibata, A.; Nagaoka, S.; Mukai, K. Kinetic study of aroxyl radical-scavenging action of vitamin E in membranes of egg yolk phosphatidylcholine vesicles. *Chem. Phys. Lipids* **2011**, *164*, 205–210.

(16) Kharasch, M. S.; Joshi, B. S. Reactions of hindered phenols. I. Reactions of 4,4'-dihydroxy-3,5,3',5'-tetra-*tert*-butyl diphenylmethane. *J. Org. Chem.* **1957**, *22*, 1435–1438.

(17) Bartlett, P. D.; Funahashi, T. Galvinoxyl (2,6-di-*tert*-butyl- α -(3,5-di-*tert*-butyl-4-oxo-2,5-cyclohexadiene-1-ylidene)-*p*-tolylxy) as a scavenger of shorter-lived free radicals. *J. Am. Chem. Soc.* **1962**, *84*, 2596–2601.

(18) Mukai, K. Anomalous magnetic properties of stable crystalline phenoxyl radicals. *Bull. Chem. Soc. Jpn.* **1969**, *42*, 40–46.

(19) Rieker, A.; Scheffler, K. Die Beteiligung von Phenylresten an der Aroxylmesomerie. *Liebigs Ann. Chem.* **1965**, *689*, 78–92.

(20) Forrester, A. R.; Hay, J. M.; Thomson, R. H. *Organic Chemistry of Stable Free Radicals*; Academic Press: London, UK, 1968; p 138.

(21) Mukai, K.; Sogabe, A. ESR studies of radical pairs of galvinoxyl radical in corresponding phenol matrix. *J. Chem. Phys.* **1980**, *72*, 598–601.

(22) Nilsson, J. L. G.; Sievertsson, H.; Selander, H. Synthesis of methyl substituted 6-hydroxychromans, model compounds of tocopherols. *Acta Chem. Scand.* **1968**, *22*, 3160–3170.

(23) Mukai, K.; Kageyama, Y.; Ishida, T.; Fukuda, K. Synthesis and kinetic study of antioxidant activity of new tocopherol (vitamin E) compounds. *J. Org. Chem.* **1989**, *54*, 552–556.

(24) Mukai, K.; Ishikawa, E.; Ouchi, A.; Nagaoka, S.; Suzuki, T.; Izumisawa, K.; Koike, T. Kinetic study of the quenching reaction of singlet oxygen by α -, β -, γ -, δ -tocotrienols and palm oil and soybean extracts in solution. *Food Funct.* **2013**, unpublished results.

(25) (a) Atkins, P.; Paula, J. In *Atkins' Physical Chemistry*, 9th ed.; Oxford: Oxford, UK, 2010. Section 21.1b. (b) Section 21.3b.

(26) Mukai, K.; Ouchi, A.; Mitarai, A.; Ohara, K.; Matsuoka, C. Formation and decay dynamics of vitamin E radical in the antioxidant reaction of vitamin E. *Bull. Chem. Soc. Jpn.* **2009**, *82*, 494–503.

(27) Ouchi, A.; Nagaoka, S.; Mukai, K. Tunneling effect in regeneration reaction of vitamin E by ubiquinol. *J. Phys. Chem. B* **2010**, *114*, 6601–6607.

(28) Mukai, K.; Watanabe, Y.; Uemoto, Y.; Ishizu, K. Stopped-flow investigation of antioxidant activity of tocopherols. *Bull. Chem. Soc. Jpn.* **1986**, *59*, 3113–3116.

(29) Mukai, K.; Tokunaga, A.; Itoh, S.; Kanesaki, Y.; Ohara, K.; Nagaoka, S.; Abe, K. Structure-activity relationship of the free-radical-scavenging reaction by vitamin E (α -, β -, γ -, δ -tocopherols) and ubiquinol-10: pH dependence of the reaction rates. *J. Phys. Chem. B* **2007**, *111*, 652–662.

(30) Mukai, K.; Daifuku, K.; Okabe, K.; Tanigaki, T.; Inoue, K. Structure-activity relationship in the quenching reaction of singlet oxygen by tocopherol (vitamin E) derivatives and related phenols. Finding of linear correlation between the rates of quenching of singlet oxygen and scavenging of peroxy and phenoxy radicals in solution. *J. Org. Chem.* **1991**, *56*, 4188–4192.

(31) Huang, D.; Ou, B.; Prior, R. L. The chemistry behind antioxidant capacity assays. *J. Agric. Food Chem.* **2005**, *53*, 1841–1856.

(32) Prior, R. L.; Wu, X.; Schaich, K. Standardized methods for the determination of antioxidant capacity and phenolics in foods and dietary supplements. *J. Agric. Food Chem.* **2005**, *53*, 4290–4302.

(33) Naqvi, K. R.; Li, H.; Melø, T. B.; Webster, R. D. Spectroscopic characterization of neutral and cation radicals of α -tocopherol and related molecules: a satisfactory denouement. *J. Phys. Chem. A* **2010**, *114*, 10795–10802.

(34) Mukai, K.; Fujii, Y.; Ishizu, K.; Kitamura, Y. A study of antioxidant activity of vitamin E derivatives by means of stopped-flow spectroscopy. Presented at the Joint Meeting of Chugoku/Shikoku and Kyusyu Branches of Chemical Society of Japan, Tokushima, Nov 1986; Paper 1D16.

(35) Žilić, D.; Pajić, D.; Jurić, M.; Molčanov, K.; Rakvin, B.; Planinić, P.; Zadro, K. Single crystals of DPPH grown from diethyl ether and carbon disulfide solutions – crystal structures, IR, EPR and magnetization studies. *J. Magn. Reson.* **2010**, *207*, 34–41 and references cited therein.

(36) Meo, F. D.; Lemaury, V.; Cornil, J.; Lazzaroni, R.; Jean-Luc Duroux, J.-L.; Olivier, Y.; Trouillas, P. Free radical scavenging by natural polyphenols: atom versus electron transfer. *J. Phys. Chem. A* **2013**, *117*, 2082–2092.

(37) Kawashima, T.; Ohkubo, K.; Fukuzumi, S. Radical scavenging reactivity of catecholamine neurotransmitters and the inhibition effect for DNA cleavage. *J. Phys. Chem. B* **2010**, *114*, 675–680 and references cited therein.

(38) Zheludev, A.; Bonnet, M.; Ressouche, E.; Schweizer, J.; Wan, M.; Wang, H. Experimental spin density in the first purely organic ferromagnet: the β para-nitrophenyl nitronyl nitroxide. *J. Magn. Magn. Mater.* **1994**, *135*, 147–160.

(39) Xiao, C.; Feng, K.; Mo, Y.; Meng, Q.; Zhang, M.; Wan, M.; Zhao, J. The electronic structure and Raman spectroscopy of the first purely organic ferromagnet: β para-nitrophenyl nitronyl nitroxide. *Chem. Phys.* **1998**, *237*, 73–79 and references cited therein.

(40) Nishide, H.; Suga, T. Organic radical battery. *Electrochem. Soc. Interface* **2005**, *14* (4), 32–36.

(41) Burton, G. W.; Doba, T.; Gabe, E. J.; Hughes, L.; Lee, F. L.; Prasad, L.; Ingold, K. U. Autoxidation of biological molecules. 4. Maximizing the antioxidant activity of phenols. *J. Am. Chem. Soc.* **1985**, *107*, 7053–7065.

(42) Pryor, W. A.; Cornicelli, J. A.; Devall, L. J.; Tait, B.; Trivedi, B. K.; Witiak, D. T.; Wu, M. A rapid screening test to determine the antioxidant potencies of natural and synthetic antioxidant. *J. Org. Chem.* **1993**, *58*, 3521–3532.

(43) Pryor, W. A.; Strickland, T.; Church, D. F. Comparison of the efficiencies of several natural and synthetic antioxidants in aqueous sodium dodecyl sulfate micelle solutions. *J. Am. Chem. Soc.* **1988**, *110*, 2224–2229.

(44) Traber, M. G.; Atkinson, J. Vitamin E, antioxidant and nothing more. *Free Radical Biol. Med.* **2007**, *43*, 4–15 (review).

(45) Leth, T.; Søndergaard, H. Biological activity of vitamin E compounds and natural materials by the resorption-gestation test, and chemical determination of the vitamin E activity in foods and feeds. *J. Nutr.* **1977**, *107*, 2236–2243.

(46) Velioglu, Y. S.; Mazza, G.; Gao, L.; Oomah, B. D. Antioxidant activity and total phenolics in selected fruits, vegetables, and grain products. *J. Agric. Food Chem.* **1998**, *46*, 4113–4117.

(47) Kähkönen, M. P.; Hopia, A. I.; Vuorela, H. J.; Rauha, J.-P.; Pihlaja, K.; Kujala, T. S.; Heinonen, M. Antioxidant activity of plant extracts containing phenolic compounds. *J. Agric. Food Chem.* **1999**, *47*, 3954–3962.